IEEE Access
Multidisciplinary | Rapid Review | Open Access Journal

Received April 26, 2020, accepted May 3, 2020, date of publication May 6, 2020, date of current version May 19, 2020.

Digital Object Identifier 10.1109/ACCESS.2020.2992700

Study on Temperature Adjustable Terahertz Metamaterial Absorber Based on Vanadium Dioxide

YUBING ZHANG[1], PINGHUI WU[2,4], ZIGANG ZHOU[1], XIFANG CHEN[1], ZAO YI[1], JIAYI ZHU[1], TIANSHENG ZHANG[3], AND HUGE JILE[3]

[1]Joint Laboratory for Extreme Conditions Matter Properties, Southwest University of Science and Technology, Mianyang 621010, China
[2]Fujian Key Laboratory for Advanced Micro-Nano Photonics Technology and Devices, Research Center for Photonic Technology, Quanzhou Normal University, Quanzhou 362000, China
[3]School of Science, Huzhou University, Huzhou 313000, China
[4]Collaborative Innovation Center for Ultra-Precision Optical Engineering and Applications, Quanzhou Normal University, Quanzhou 362000, China

Corresponding authors: Zao Yi (yizaomy@swust.edu.cn), Jiayi Zhu (jyzhu@swust.edu.cn), and Huge Jile (hgjl@zjhu.edu.cn)

This work was supported in part by the National Natural Science Foundation of China (NNSFC), under Grant 51606158, Grant 11604311, Grant 11875297, Grant 21506257, Grant 11704223, Grant 11947410, and Grant 51575407, in part by the Natural Science Foundation of Fujian Province under Grant 2018J05008 and Grant JZ160459, in part by the Sichuan Science and Technology Program under Grant 2018GZ0521, in part by the Ph.D. Research Startup Foundation of Quanzhou Normal University under Grant G16057, in part by the Distinguished Young Scholars Program of Fujian Province under Grant C18032, in part by the Undergraduate Innovation Fund Project Precision Funding by the Southwest University of Science and Technology under Grant JZ-19058, and in part by the Postgraduate Innovation Fund Project by Southwest University of Science and Technology under Grant 19ycx0067.

ABSTRACT In the study of modern optics, the work of terahertz metamaterial absorbers is mostly multi-band perfect absorbers and ultra-wideband perfect absorbers. In contrast, in practical applications, metamaterial absorbers with adjustable resonance frequency or amplitude play an essential role in many forms. Here, we firstly designed an ultra-wideband terahertz metamaterial perfect absorber, achieving over 99% perfect absorption in the 6.6-8.9 THz range. Secondly, based on the absorber, phase change material VO_2 was added to improve the structure, and three tunable terahertz metamaterial absorbers based on VO_2 were designed, respectively realizing broadband movement and conversion between broadband and multi-band. Also, the terahertz absorber with dynamic tuning characteristics can flexibly control the absorption performance, providing an excellent platform for the realization of terahertz filtering, modulation, and so on.

INDEX TERMS Broadband, multiband, active tuned, vanadium dioxiderption, high quality factor.

I. INTRODUCTION

At present, the use of photoelectric methods to realize the dynamic and controllable characteristics of metamaterials has attracted more and more attention from experts. Vanadium dioxide, like a phase change material, it is well known that the transition from insulation state to metal state can achieve at 340 K temperature [1]–[4]. With the rise of heat, the lattice structure of vanadium dioxide gradually changed from a monoclinic structure to a four-angle structure, and its conductivity increased steadily in the process of temperature rise [5]–[9]. Therefore, based on the above characteristics, vanadium dioxide has been widely used in the development of thermal responsive photonic electronics and thermal equipment [10], [11].

The associate editor coordinating the review of this manuscript and approving it for publication was Sukhdev Roy.

In recent years, active and tunable absorbers have received more and more attention [12]–[21]. However, some adjustment methods still need to change some conditions for implementation artificially. So how to achieve true active tunability is a significant development direction of metamaterial absorbers now. In 2010, Huang *et al.* made a metal gold/vanadium dioxide gasket/metal gold composite metamaterial to study the mechanism of the light response. They found that the nanostructures, with vanadium dioxide pads, could be used as dynamic light switches for temperature control [22]. In 2012, Katsetal made a nanoscale metamaterial device that used a thin film layer of vanadium dioxide with a loss of dielectric constant much smaller than the incident wavelength on the sapphire substrate to achieve perfect absorption.

Moreover, the light absorption of 99.75% was realized near the nonmetallic-metallic phase transition of vanadium

dioxide itself [23]. In 2015, Kocer *et al.* made a heat-adjustable short-wave infrared resonance absorber by heating the hybrid alloy-vanadium dioxide nanostructure array above the phase transition temperature of vanadium dioxide [24]. In 2017, Zhu *et al.* generated a ''bow-tie'' type periodic cell structure and connected vanadium dioxide blocks at the feed point of a single structure to make a surface metamaterial efficient absorber. Experimental results indicate that the structure can achieve an adjustable bandwidth of 360 nm in the near-infrared region. In the terahertz frequency region, the conductivity of vanadium dioxide varies by orders of magnitude following a phase transition [25]. In 2019, the sailors designed a terahertz absorber consisting of a circular resonant ring structure with the electromagnetic response to four frequency bands. The terahertz multi-band absorber was designed and simulated by changing the geometric size of the top metal ring pattern, the dielectric thickness of the middle layer, and the conductivity change rate of the photosensitive silicon at the top metal ring [26]. In the same year, Xia *et al.* designed a photonic crystal structure of the doped silicon with absorption effect is designed to achieve wide-band absorption in the 0.29 to 0.31 THz band, and the photonic crystal has a significant effect on the thermo-optic effect, thereby achieving the function of temperature adjustment [27]. In 2019, Wei *et al.* designed a large-angle mid-infrared absorption switch by introducing the phase change material GST [28]. In 2020, Song *et al.* proposed a multi-layer metamaterial with switchable function based on the phase change characteristics of vanadium dioxide. The combination of the two absorption peaks can make the absorption rate in the wide spectral range of 0.393 THz to 0.897 THz more than 90%. In addition, the research group proposed multi-layer vanadium dioxide-based metamaterial with dual functional properties of absorption and polarization conversion, which can convert linear plane waves into their corresponding cross-polarized waves at 2.0-3.0 THz. The frequency is more than 90% efficient [29], [30].

In this paper, an ultra-wideband terahertz metamaterial absorber is proposed, in which the absorption layer is composed of four T-shaped structures, achieving over 99% perfect absorption in the range of 6.6 THz to 8.9 THz. The mechanism of broadband absorption is analyzed by drawing the electric field and current density diagrams at various frequencies. Besides, we introduced a vanadium dioxide, a phase change material based on a broadband metamaterial absorber. In addition, the basic structure is improved, and three arrangements are designed to realize an active tunable terahertz metamaterial absorber. Its three structures are VO_2-silica-gold-VO_2-silica-gold, gold-silica-VO_2-silica, gold-silica-VO_2-gold. Also, it is proved by simulation that the three structures above can make the absorption bandwidth of the original absorber rise and fall, transfer, and transform the super-bandwidth absorption into multi-band absorption. This actively tunable terahertz metamaterial absorber plays a vital role in many practical applications.

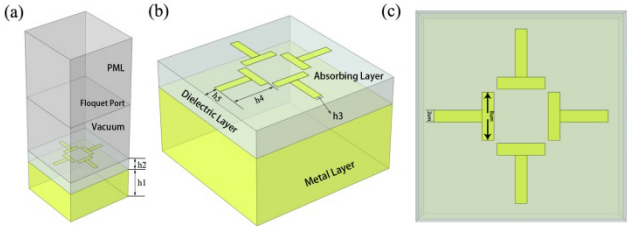

FIGURE 1. Schematic diagram of the base absorber : (a) one unit structure of the absorber, (b) main components of the absorber, and (c) schematic diagram of the absorption layer.

II. DESIGN, SIMULATION, EXPERIMENT, AND THEORY

The model structure of the primary uwb terahertz metamaterial absorber is shown in figure 1. The absorber continues the basic metal-dielectric-metal structure [31]–[35]. In the absorber, the metal materials are all gold, and the conventional silica is selected as the medium material. In the final designed structure, from bottom to top, there are the reflection layer, the medium layer and the absorption layer, with the thickness $h1$=16 um, $h2$=6.34 um and $h3$=0.05 um, respectively, and the period P of the absorber is set as 35 um. The tod of four T-shaped structures, and each T-shaped structure is composed of two rectangles of the same sizep absorption layer is compose. The length and width of the boses are 8 um and 2 um, respectively. The distance between the top of the corresponding T-shaped structure and the bottom of the T-shaped structure is $h4$=9 um, and the gap between the tail of the T-shaped structure and the bottom of the absorber is $h5$=3 um. In the selection of material properties, the relevant parameters of gold are represented by the Drude model, and the relative permittivity of silica in the dielectric layer was set as 2.13. We use a finite element method for modeling (COMSOL). We set the boundary conditions of the metamaterial absorber to Floquet. The periodic boundary and the Floquet regular port allow the metamaterial absorber we design to become an infinite array in space. In the process of simulation, the gold at the bottom can well block the incident light, and the transmission (T) of the structure is almost 0 (T=0). So absorption can be expressed as A=1-R (reflection) [36]–[40].

In the basic structure, the basic principle is to minimize the reflection coefficient by matching the impedance with the free space and eliminate the transmittance by maximizing the metamaterial loss. The top of the periodic array of metal array structure for a metamaterial structure absorbing ability is essential, when the electromagnetic wave incident to metamaterials structure of the upper metal structure, because of its particular geometric parameters and geometry structure, will take place at a particular frequency electromagnetic resonance, based on the Drude model, real ε_1 and imaginary part of dielectric constant ε_2 can be expressed as [42], [43]:

$$\varepsilon_{1(\omega)} = \varepsilon_\infty - \frac{\omega_p^2 \tau^2}{1 + \omega^2 \tau^2} \tag{1}$$

$$\varepsilon_{2(\omega)} = \omega\tau \frac{\omega_p^2 \tau^2}{1 + \omega^2 \tau^2} \tag{2}$$

Angular frequency of the incident electromagnetic wave ω, ω_p is plasma frequency, τ as the relaxation time, ε_∞ for Drude constant. When $\omega\tau \gg 1$, a dielectric constant real component can be represented as:

$$\varepsilon_{1(\omega)} = \varepsilon_\infty - \frac{\omega_p^2}{\omega^2} \tag{3}$$

From the above equation, we can see that as $\boldsymbol{\varepsilon}$ approaches infinity, the real part of the permittivity is $\boldsymbol{\varepsilon}_\infty$. $\boldsymbol{\varepsilon}_\infty$ reflect the contribution from the polarization of the inner electrons.

In addition to generating resonance, the periodic metal structure array at the top of the infrastructure has another critical function, which is to form impedance matching. By matching the impedance of the structure array with the free space, the reflection of the electromagnetic waves on the surface of the metamaterial absorbing structure can be zero. Such impedance matching can be achieved through specific resonance or plasmon coupling, and metamaterials can be regarded as homogeneous materials at a macroscopic level. The medium layer in the middle of the infrastructure is mainly used to provide space for the electromagnetic wave incident into the absorption structure and absorb the event electromagnetic wave. For ordinary absorbers, to give enough absorption space for electromagnetic waves, materials with relatively sizeable refractive index are generally used to reduce the thickness of the dielectric layer. However, for the absorption structure of metamaterials, the effect of the dielectric layer is not only limited to the absorption of electromagnetic waves but also the electromagnetic resonance satisfying the structure of metamaterials.

In this paper, only the simulation results are considered, and the critical processes for the preparation of the structure are described as follows: (I) liquid phase method or molecular beam epitaxy (MBE) for the preparation of VO_2 films. (II) preparation of gold arrays by electric beam evaporation and ultraviolet (UV) lithography; (III) make dielectric layer 2; (IV) preparation of a VO_2 array by UV lithography and subsequent reactive ion etching.

III. RESULTS AND DISCUSSION

A. ABSORPTION CURVE AND MECHANISM OF INFRASTRUCTURE

Figure 2 shows the absorption curve of the absorber under the foundation structure. We can find in the absorber in 6.5-8.95 THz frequency range you have incredibly high broadband absorption, within the scope of the average absorption can reach more than 98.6%, and 99.9% in many places have high absorption. Compared with other people's work, the absorption bandwidth has been greatly improved, as shown in table 1 [44]–[48]. To this, we combine the absorber in figure 3 electric field, and current density distribution on the absorption mechanism of the absorber are studied.

In figure 3, we give the distribution of electric field and current density at 7, 8, and 9 THz, respectively. In figure 3, it can be known that the reason for broadband absorption is mainly caused by the resonance coupling of four T-shaped structures. However, due to the influence of polarization

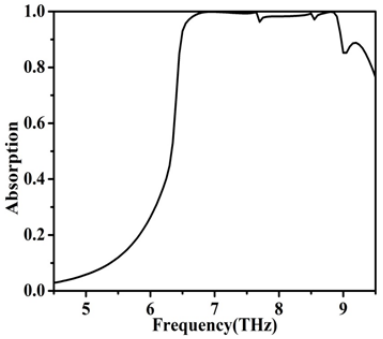

FIGURE 2. The absorption curve of the absorber in the range of 4.5-9.5 THz when the incident angle is 20°.

TABLE 1. Some latest information on VO_2 absorbents.

Refer	type of absorber	Absorption band-width	Modulation depth
[42]	Ultra-broadband THz Absorber	1.63-3.86 THz	Over 90%
[43]	Ultra-broadband near-infrared absorber	1.2-2.5 μm	Over 90%
[44]	Ultra-broadband THz absorber	10.28-15.56 THz	Over 90%
[45]	Dual broadband THz absorber	0.56-1.44 THz and 2.88-3.65 THz	Over 80%
[46]	Broadband THz absorber	1.05-1.6 THz	Over 90%
Present	Ultra-broadband THz Absorber	6.6-8.9 THz	Over 90%

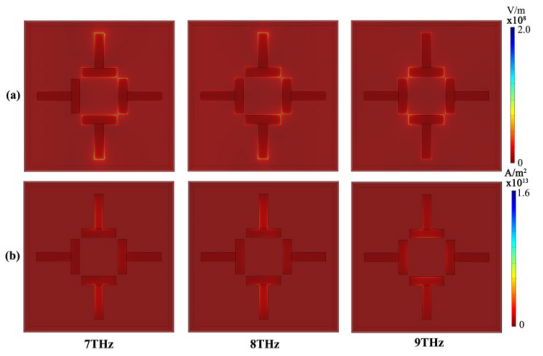

FIGURE 3. (a) and (b) Show the electric field density and surface current distribution of the absorber of 7 THz, 8THz, and 9.00 THz, respectively.

direction, the resonance of two T-shaped structures in the vertical direction is relatively stable and prominent. In contrast, the resonance coupling in the horizontal direction is relatively small. When the electric field at these three frequencies and the current surface diagram are respectively corresponding to the absorption curve, we can better explain the absorption reasons. At 7 and 8 THz, we can find that both the top and the tail of the T-shaped have strong electric fields, while at 9 THz, the generated electric fields mainly exist at the junction of the T-shaped, so the absorption at 9 THz is lower than other places. Also, by observing the current distribution and the pointing vector of the surface current, we can find that the

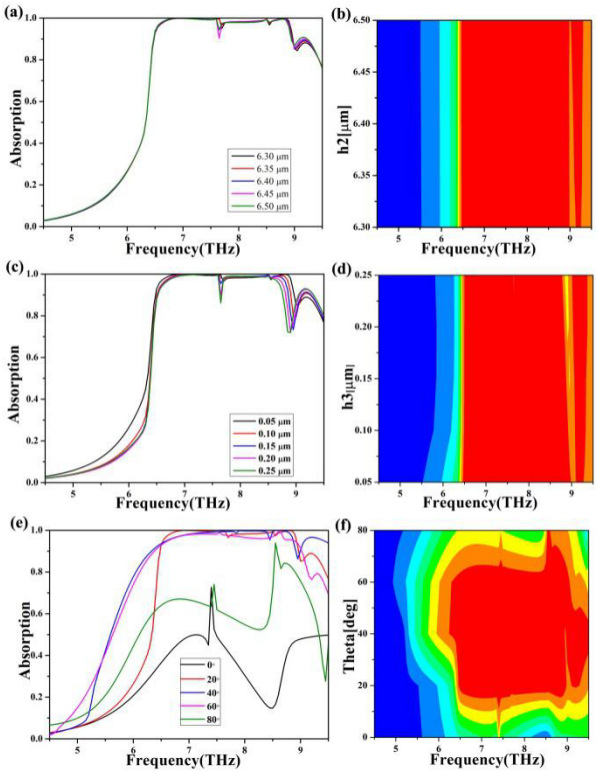

FIGURE 4. The absorption images of the scanning dielectric layer thickness (are shown in (a) and (b)). The absorption images of the scanning absorption layer thickness are shown in (c) and (d). The absorption images of the scanning different angles of incidence (0-80°) are shown in (e) and (f).

current loop can be formed between the four T characters at 7 and 8 THz. In contrast, the current flow at the front end of only T character is steady at 9 THz.

Considering the errors that may occur in the actual manufacturing process of the structure, we continue to analyze the influence of the structural parameters on the resonance. In figure 4, we plot the thickness of the different dielectric layers, the width of the absorbing layer, and the absorption layer when the incident angle is altered. When the thickness of the dielectric layer is changed, the absorption curve has a significant red shift phenomenon. However, when we change the thickness of the absorber dielectric layer in a smaller range, the absorber still has high broadband absorption characteristics, as shown in figure 4 (a) and (b). As can be seen from figure 4 (c) and (d), the absorption value gradually decreases with the increase of the absorption layer thickness. This is because metal materials can support the SPP in visible light, but higher losses and shorter propagation distances will reduce the mass of surface waves. In addition, the absorption rate increases with the increase of incidence angle. This is because as the incident angle increases, the absorption gradually increases. At first, as the reflection of electromagnetic waves increases under high oblique incidence, the absorption decreases with increasing angle. Then, when the incident angle is increased, the magnetic dipole oscillation of the entire absorber is efficiently excited, so that strong absorption characteristics are maintained at large angles. Generally, the absorber has a good absorption effect on electromagnetic waves with a broader incident angle. Therefore, in the actual structure preparation process, the effects of layer thickness and cell size on the resonance peaks are small.

B. ABSORPTION CURVE AND MECHANISM OF VO_2 ABSORBER

We can use the Drude model to describe the optical dielectric constant of vanadium dioxide in the terahertz band [49]–[53]:

$$\varepsilon(\omega) = \varepsilon_\infty - \frac{\omega_\rho^2(\sigma)}{\omega^2 + i\gamma\omega} \tag{4}$$

where $\varepsilon_\infty = 12$ is the relative dielectric constant of vanadium dioxide at high frequencies, $\omega_\rho^2(\sigma)$ is the conductance dependent plasma frequency, and γ is the damping frequency. In addition, we can see that $\omega_\rho^2(\sigma)$ and σ are proportional to the carrier density in the free space. Therefore, the plasma frequency can be approximated as an expression.

$$\omega_\rho^2(\sigma) = \frac{\sigma}{\sigma_0}\omega_\rho^2(\sigma_0) \tag{5}$$

where $\sigma_0 = 3*10^3 \Omega$/cm, $\omega_\rho(\sigma_0) = 1.5*10^{15}$ rad/s, $\gamma = 5.75*10^{13}$ rad/s. In the terahertz band, we use parameters such as changing the structural size of the top metal of the absorber to achieve impedance matching between the dielectric layer of the electromagnetic metamaterial absorber and free space. That is, we can adjust the parameters ε and μ simultaneously. In this way, we can make them match the impedance $z = \sqrt{\mu/\varepsilon}$ of free space. In this way, the reflectance can be reduced in a specific frequency band. When the change of external temperature causes the phase transition of vanadium dioxide, the conductivity of vanadium dioxide changes accordingly, thus breaking the impedance matching with the original structure and the space medium layer, so that the electromagnetic wave is strongly reflected, resulting in the decline of absorption. Similarly, when the temperature conditions remain unchanged, the thickness of vanadium dioxide decreases, and the electromagnetic wave transmission increases, which also leads to the absorption decline. We plot the relationship between conductivity and temperature, as shown in figure 5.

According to the relationship between the dielectric function of the material and the electrical conductivity, we can get the electrical conductivity relationship of the VO_2 film at different temperatures during the phase transition as [54]–[56]:

$$\sigma = -i\varepsilon_0\omega(\varepsilon_C - 1) \tag{6}$$

Among them, σ is the conductivity of the composite system, ε_0 is the dielectric constant of the vacuum, and the dielectric function ε_C of the composite system is related to temperature. We offer the relationship between temperature and conductivity, and here we give several corresponding values. At 313 K, the conductivity is 130 S/m; at 333 K, the conductivity is 820 S/m; at 340 K, the conductivity is 21700 S/m; at 342 K, the conductivity is 158000 S/m; at 353 K, the final conductivity is 212000 S/m.

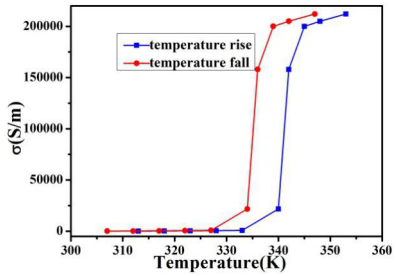

FIGURE 5. Schematic diagram of the relationship between conductivity and temperature.

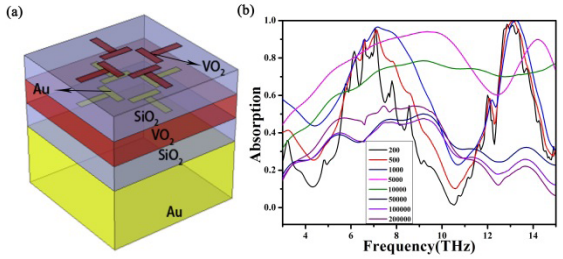

FIGURE 6. (a) Is the main component of structure I type vanadium dioxide metamaterial absorber, (b) is the absorption curve of structure 1 type vanadium dioxide metamaterial absorber.

C. STRUCTURAL TYPE I VANADIUM DIOXIDE METAMATERIAL ABSORBER

Figure 6 (a) shows that we add two more layers of VO_2 and one layer of SiO_2 to the basic structure. The model of VO_2 terahertz metamaterial active tunable absorber was established. We call it to structure I-vanadium dioxide metamaterial absorber. The structure from top to bottom is a periodic array layer composed of VO_2, a dielectric layer (I), a periodic array layer composed of gold, a VO_2 layer, a dielectric layer (II), and a final layer of Au. To make the absorber have dynamic and adjustable absorption characteristics, we have added two layers of VO_2 to the previously designed primary absorber. One layer is designed for a specific unit structure, and the other layer acts as a dielectric layer. VO_2 can change the internal lattice structure through some effects such as light and heat so that it can be transformed from the insulating phase to the metal phase. In the tunable structure we designed, the conductivity of VO_2 can be controlled by light, so that the temperature change can be controlled. In addition, this structure is equivalent to adding a dielectric layer and an absorption layer, so it is equal to combining two absorbers together. When the temperature of the absorber is higher than the phase transition temperature of VO_2, VO_2 is in the metal phase at this time, and the effect is similar to Au. At this time, it is equivalent to the role of a metal mirror. Light does not pass through this layer structure so that the following structure can be ignored. At this time, the structure only has the top three layers functioning to form an absorber. The active part of the structure is the VO_2 periodic array, the dielectric layer (I), and the VO_2 layer. When the temperature of the absorber is lower than the phase transition temperature of VO_2, then VO_2 is in the insulating phase. Therefore, VO_2 used in this structure can be considered as a dielectric layer. At this time, the absorbed multilayer structure is similar to the three-layer primary structure in the basic absorber. Therefore, we can control the phase change of VO_2 by adding VO_2 to the central absorber and then realize the active tunable absorption of the absorber.

From the above analysis, we know that temperature affects the conductivity of VO_2, so we draw the absorption curve pattern with the change of conductivity of the absorption under this structure in figure 6 (b). By observing the absorption curve, we can discover that the absorber produces several chaotic absorption peaks when the conductivity is low, and the position of the absorption peak is consistent with that of the infrastructure. However, as the gradual increase of the conductivity, the absorption peak gradually improves. When the conductivity is 500, the absolute absorption peak appears at 2 THz. When the conductivity then rises high enough, we have broadband absorption in the absorber, and broadband is much broader than in the previous infrastructure.

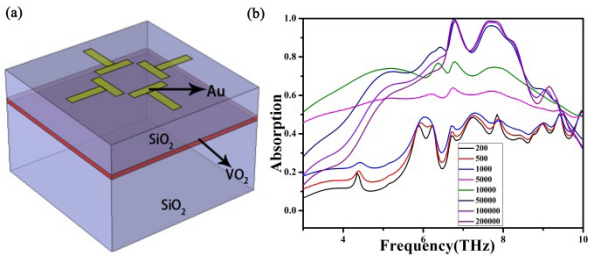

FIGURE 7. (a) Is the main component of structure II type vanadium dioxide metamaterial absorber, (b) is the absorption curve of structure 2 type vanadium dioxide metamaterial absorber.

D. STRUCTURAL TYPE II VANADIUM DIOXIDE METAMATERIAL ABSORBER

Figure 7 (a) is a schematic diagram of a structural II VO_2 terahertz metamaterial active adjustable absorber. This structure adds a layer of VO_2 to the construction of the original absorber and replaces the metal material at the bottom with a dielectric material. From top to bottom, the periodic array layer-dielectric layer-VO_2 layer-point dielectric layer is composed of gold. When the temperature of VO_2 is low, the structure is equivalent to a metal-dielectric structure and still absorbs part of the incident light. However, since the bottom is made of a dielectric material, projected light is generated. When the temperature of VO_2 rises to the phase transition temperature, the structure is equivalent to a base formed by adding a dielectric layer under the original base structure, and the influence on the absorption curve is not significant.

The absorption curve under this structure is shown in figure 7 (b). We can find that when the temperature is low, the absorption value is shallow due to the presence of transmitted light in this absorber, but it can still be equivalent to

a broadband absorption of 40%-50% at 6-10 THz. As the temperature increases (that is, the conductivity increases), we can see that absorption increases significantly. At conductivity of 10000, there is more than 70% broadband absorption at 4-9 THz. When VO_2 is completely transformed into the metallic phase, it is evident that the structural absorber has an absolute absorption peak and a small broadband generation. Comparing the absorption peak with the frequency of the absorption broadband, we find that the absorption peak is before 6.5-9 THz, which is in perfect agreement with our previous infrastructure.

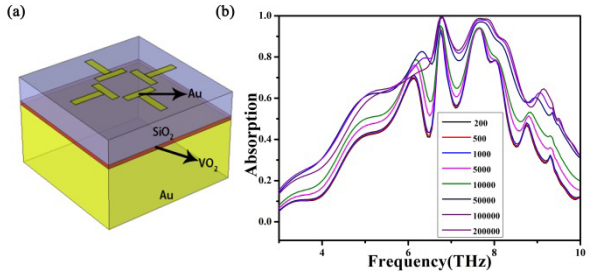

FIGURE 8. **(a) Is the main component of structure III type vanadium dioxide metamaterial absorber, (b) is the absorption curve of structure 3 type vanadium dioxide metamaterial absorber.**

E. STRUCTURAL TYPE III VANADIUM DIOXIDE METAMATERIAL ABSORBER

Figure 8 (a) is a model diagram of a structural III VO_2 terahertz metamaterial active adjustable absorber. The junction is somewhat similar to structure II, in that it is made up of a layer of VO_2 on top of the original infrastructure, but the material at the bottom is still gold, and the periodic array layer from top to bottom is Au-dielectric layer-VO_2 layer-Au layer. When the temperature of VO_2 is low, the structure is equivalent to a metal-dielectric-metal structure, which is very similar to the basic structure. However, because the relative dielectric constants of VO_2 and SiO_2 are not the same, the dielectric layer formed by the combination of the two is also thicker than the basic structure, so the resonance absorption generated will also be very different from that before. When the temperature of VO_2 rises to the phase transition temperature, the structure is equivalent to that VO_2 forms a reflective metal layer together with gold at the bottom, so the absorption is somewhat similar to that of structure II.

The absorption curve under the absorber is shown in figure 8 (b). We can find that when the electrical conductivity of the absorber is low, the absorber when in the dual-band terahertz metamaterial absorber, but absorption value is not high, the dielectric layer and absorbing layer to produce resonance mode, when the conductivity increased VO_2, absorption curve and structure can be found two absorption curve is similar, this is because at this point, the structure of two and three structure at the top of the absorbing layer and in the middle of the dielectric layer is entirely consistent. The order of the VO_2 with Au layer under the influence on absorption is not very big, mainly have the effect of absorption of transmitted light.

IV. CONCLUSIONS

To sum up, we firstly designed an ultra-wideband terahertz metamaterial perfect absorber, which achieved over 99% perfect absorption within the range of 6.6-8.9 THz, and mapped the surface electric field and surface current density distribution to study the absorption mechanism. Secondly, based on the absorber, phase change material VO_2 was added to improve the structure, and three tunable terahertz metamaterial absorbers based on VO_2 were designed, respectively realizing broadband movement and conversion between broadband and multi-band. In addition, the terahertz absorber with dynamic tuning characteristics can flexibly control the absorption performance, providing an excellent platform for the realization of terahertz filtering, modulation, and so on.

AUTHOR CONTRIBUTIONS

Conceptualization, Y.Z., P.W., and Z.Y.; data curation, Y.Z., P.W., and X.C.; formal analysis, Z.Y., J.Z., Z.Z., P.W., and T.Z.; methodology, Z.Z., P.W., and T.Z.; resources, P.W.; software, P.W., Z.Z., T.Z., and H.J.; data curation, Y.Z.; writing—original draft preparation, T.Z.; Y.Z. writing—review and editing, Y.Z., P.W., Z.Y., X.C., and J.Z. All authors have read and agreed to the published version of the manuscript.

FUNDING

This research received no external funding.

ACKNOWLEDGMENT

(Yubing Zhang and Pinghui Wu contributed equally to this work.)

CONFLICTS OF INTERES

The authors declare no conflicts of interest.

REFERENCES

[1] H. Luo, Q. Li, K. Du, Z. Xu, H. Zhu, D. Liu, L. Cai, P. Ghosh, and M. Qiu, "An ultra-thin colored textile with simultaneous solar and passive heating abilities," *Nano Energy*, vol. 65, Nov. 2019, Art. no. 103998.

[2] P. Wu, Z. Chen, H. Jile, C. Zhang, D. Xu, and L. Lv, "An infrared perfect absorber based on metal-dielectric-metal multi-layer films with nanocircle holes arrays," *Results Phys.*, vol. 16, Mar. 2020, Art. no. 102952.

[3] M. Pan, Y. Huang, Q. Li, H. Luo, H. Zhu, S. Kaur, and M. Qiu, "Multi-band middle-infrared-compatible camouflage with thermal management via simple photonic structures," *Nano Energy*, vol. 69, Mar. 2020, Art. no. 104449.

[4] Z. Xu, Q. Li, K. Du, S. Long, Y. Yang, X. Cao, H. Luo, H. Zhu, P. Ghosh, W. Shen, and M. Qiu, "Spatially resolved dynamically reconfigurable multilevel control of thermal emission," *Laser Photon. Rev.*, vol. 14, no. 1, Jan. 2020, Art. no. 1900162.

[5] M. Liu, H. Y. Hwang, H. Tao, A. C. Strikwerda, K. Fan, G. R. Keiser, A. J. Sternbach, K. G. West, S. Kittiwatanakul, J. Lu, S. A. Wolf, F. G. Omenetto, X. Zhang, K. A. Nelson, and R. D. Averitt, "Terahertz-field-induced insulator-to-metal transition in vanadium dioxide metamaterial," *Nature*, vol. 487, no. 7407, pp. 345–348, Jul. 2012.

[6] W. Wang, Y. Qu, K. Du, S. Bai, J. Tian, M. Pan, H. Ye, M. Qiu, and Q. Li, "Broadband optical absorption based on single-sized metal-dielectric-metal plasmonic nanostructures with high-ϵ' metals," *Appl. Phys. Lett.*, vol. 110, no. 10, Mar. 2017, Art. no. 101101.

[7] Z. Zhou, J. Li, Z. Xiong, L. Cao, Y. Fu, and Z. Gao, "Reducing transition temperature and diluting brown-yellow color of VO2 films via embedding ag particles periodic arrays," *Sol. Energy Mater. Sol. Cells*, vol. 206, Mar. 2020, Art. no. 110303.

[8] R. M. Briggs, I. M. Pryce, and H. A. Atwater, "Compact silicon photonic waveguide modulator based on the vanadium dioxide metal-insulator phase transition," *Opt. Express*, vol. 18, no. 11, p. 11192, May 2010.

[9] Y. Qu, Q. Li, L. Cai, M. Pan, P. Ghosh, K. Du, and M. Qiu, "Thermal camouflage based on the phase-changing material GST," *Light, Sci. Appl.*, vol. 7, no. 1, p. 26, Dec. 2018.

[10] Y. Wang, Z. Chen, D. Xu, Z. Yi, X. Chen, J. Chen, Y. Tang, P. Wu, G. Li, and Y. Yi, "Triple-band perfect metamaterial absorber with good operating angle polarization tolerance based on split ring arrays," *Results Phys.*, vol. 16, Mar. 2020, Art. no. 102951.

[11] Y. Cheng, J. Fan, H. Luo, F. Chen, N. Feng, X. Mao, and R. Gong, "Dual-band and high-efficiency circular polarization conversion via asymmetric transmission with anisotropic metamaterial in the terahertz region," *Opt. Mater. Express*, vol. 9, no. 3, p. 1365, Mar. 2019.

[12] P. Wu, C. Zhang, Y. Tang, B. Liu, and L. Lv, "A perfect absorber based on similar Fabry–Pérot four-band in the visible range," *Nanomaterials*, vol. 10, no. 3, p. 488, 2020.

[13] Y. Wang, F. Jiang, J. Chen, X. Sun, T. Xian, and H. Yang, "*In situ* construction of CNT/CuS hybrids and their application in photodegradation for removing organic dyes," *Nanomaterials*, vol. 10, no. 1, p. 178, 2020.

[14] Z. Cheng and Y. Cheng, "A multi-functional polarization convertor based on chiral metamaterial for Terahertz waves," *Opt. Commun.*, vol. 435, pp. 178–182, Mar. 2019.

[15] Z. Song, A. Chen, J. Zhang, and J. Wang, "Integrated metamaterial with functionalities of absorption and electromagnetically induced transparency," *Opt. Express*, vol. 27, no. 18, p. 25196, Sep. 2019.

[16] C. Cen, Y. Zhang, X. Chen, H. Yang, Z. Yi, W. Yao, Y. Tang, Y. Yi, J. Wang, and P. Wu, "A dual-band metamaterial absorber for graphene surface plasmon resonance at terahertz frequency," *Phys. E, Low-Dimensional Syst. Nanostruct.*, vol. 117, Mar. 2020, Art. no. 113840.

[17] C. Liang, Z. Yi, X. Chen, Y. Tang, Y. Yi, Z. Zhou, X. Wu, Z. Huang, Y. Yi, and G. Zhang, "Dual-band infrared perfect absorber based on a Ag-Dielectric-Ag multilayer films with nanoring grooves arrays," *Plasmonics*, vol. 15, no. 1, pp. 93–100, Feb. 2020.

[18] S. Guan, H. Yang, X. Sun, and T. Xian, "Preparation and promising application of novel $LaFeO_3$/BiOBr heterojunction photocatalysts for photocatalytic and photo-fenton removal of dyes," *Opt. Mater.*, vol. 100, Feb. 2020, Art. no. 109644.

[19] Y. Qi, P. Zhou, T. Zhang, X. Zhang, Y. Wang, C. Liu, Y. Bai, and X. Wang, "Theoretical study of a multichannel plasmonic waveguide notch filter with double-sided nanodisk and two slot cavities," *Results Phys.*, vol. 14, Sep. 2019, Art. no. 102506.

[20] P. Ma, J. Li, H. Zhang, and Z. Yang, "Preparation of high-damage threshold WS2 modulator and its application for generating high-power large-energy bright-dark solitons," *Infr. Phys. Technol.*, vol. 105, Mar. 2020, Art. no. 103257.

[21] K. Niu, R. Sun, Q. Chen, B. Man, and H. Zhang, "Passively mode-locked er-doped fiber laser based on SnS_2 nanosheets as a saturable absorber," *Photon. Res.*, vol. 6, no. 2, p. 72, Feb. 2018.

[22] W.-X. Huang, X.-G. Yin, C.-P. Huang, Q.-J. Wang, T.-F. Miao, and Y.-Y. Zhu, "Optical switching of a metamaterial by temperature controlling," *Appl. Phys. Lett.*, vol. 96, no. 26, Jun. 2010, Art. no. 261908.

[23] M. A. Kats, D. Sharma, J. Lin, P. Genevet, R. Blanchard, Z. Yang, M. M. Qazilbash, D. N. Basov, S. Ramanathan, and F. Capasso, "Ultra-thin perfect absorber employing a tunable phase change material," *Appl. Phys. Lett.*, vol. 101, no. 22, Nov. 2012, Art. no. 221101.

[24] H. Kocer, S. Butun, B. Banar, K. Wang, S. Tongay, J. Wu, and K. Aydin, "Thermal tuning of infrared resonant absorbers based on hybrid gold-VO2 nanostructures," *Appl. Phys. Lett.*, vol. 106, no. 16, Apr. 2015, Art. no. 161104.

[25] A. V. Pogrebnyakov, J. A. Bossard, J. P. Turpin, J. D. Musgraves, H. J. Shin, C. Rivero-Baleine, N. Podraza, K. A. Richardson, D. H. Werner, and T. S. Mayer, "Reconfigurable near-IR metasurface based on $Ge_2Sb_2Te_5$ phase-change material," *Opt. Mater. Express*, vol. 8, no. 8, p. 2264, Aug. 2018.

[26] Q. Chu, M. Yang, Z. Chen, H. Zhang, X. Song, Y. Ye, Y. Ren, Y. Zhang, and J. Yao, "Characteristics of tunable Terahertz multi-band absorber," *Chin. J. Lasers*, vol. 46, no. 12, 2019, Art. no. 011482.

[27] Z. Chen, B. Liang, and S. Zhuang, "Study on photonic crystal-based temperature sensor at Terahertz band," *Optical. Instruments.*, vol. 41, no. 1, pp. 51–55, 2019.

[28] M. Wei, Z. Song, Y. Deng, Y. Liu, and Q. Chen, "Large-angle mid-infrared absorption switch enabled by polarization-independent GST meta-surfaces," *Mater. Lett.*, vol. 236, pp. 350–353, Feb. 2019.

[29] Z. Song, A. Chen, and J. Zhang, "Terahertz switching between broadband absorption and narrowband absorption," *Opt. Experss*, vol. 28, no. 2, p. 2037, Jan. 2020.

[30] M. Zhang, J. Zhang, A. Chen, and Z. Song, "Vanadium dioxide-based bifunctional metamaterial for terahertz waves," *IEEE Photon. J.*, vol. 12, no. 1, pp. 1–9, Feb. 2020.

[31] P. Yu, X. Chen, Z. Yi, Y. Tang, H. Yang, Z. Zhou, T. Duan, S. Cheng, J. Zhang, and Y. Yi, "A numerical research of wideband solar absorber based on refractory metal from visible to near infrared," *Opt. Mater.*, vol. 97, Nov. 2019, Art. no. 109400.

[32] Y. Wang, F. Qin, Z. Yi, X. Chen, Z. Zhou, H. Yang, X. Liao, Y. Tang, W. Yao, and Y. Yi, "Effect of slit width on surface plasmon resonance," *Results Phys.*, vol. 15, Dec. 2019, Art. no. 102711.

[33] F. Qin, Z. Chen, X. Chen, Z. Yi, W. Yao, T. Duan, P. Wu, H. Yang, G. Li, and Y. Yi, "A tunable triple-band near-infrared metamaterial absorber based on au nano-cuboids array," *Nanomaterials*, vol. 10, no. 2, p. 207, 2020.

[34] H. Zou and Y. Cheng, "Design of a six-band Terahertz metamaterial absorber for temperature sensing application," *Opt. Mater.*, vol. 88, pp. 674–679, Feb. 2019.

[35] Y. Cheng, J. Fan, H. Luo, and F. Chen, "Dual-band and high-efficiency circular polarization convertor based on anisotropic metamaterial," *IEEE Access*, vol. 8, pp. 7615–7621, 2020.

[36] H. Huan, H. Jile, Y. Tang, X. Li, Z. Yi, X. Gao, X. Chen, J. Chen, and P. Wu, "Fabrication of ZnO@Ag@Ag_3PO_4 ternary heterojunction: Superhydrophilic properties, antireflection and photocatalytic properties," *Micromachines*, vol. 11, no. 3, p. 309, 2020.

[37] F. Qin, X. Chen, Z. Yi, W. Yao, H. Yang, Y. Tang, Y. Yi, H. Li, and Y. Yi, "Ultra-broadband and wide-angle perfect solar absorber based on TiN nanodisk and ti thin film structure," *Sol. Energy Mater. Sol. Cells*, vol. 211, Jul. 2020, Art. no. 110535.

[38] Z. Kou, C. Miao, P. Mei, Y. Zhang, X. Yan, Y. Jiang, and W. Xiao, "Enhancing the cycling stability of all-solid-state lithium-ion batteries assembled with $Li_{1.3}Al_{0.3}Ti_{1.7}(PO_4)_3$ solid electrolytes prepared from precursor solutions with appropriate pH values," *Ceram. Int.*, vol. 46, no. 7, pp. 9629–9636, May 2020.

[39] Y. Wang, H. Yang, X. Sun, H. Zhang, and T. Xian, "Preparation and photocatalytic application of ternary n-BaTiO3/Ag/p-AgBr heterostructured photocatalysts for dye degradation," *Mater. Res. Bull.*, vol. 124, Apr. 2020, Art. no. 110754.

[40] R. Li, C. Miao, M. Zhang, and W. Xiao, "Novel hierarchical structural SnS2 composite supported by biochar carbonized from chewed sugarcane as enhanced anodes for lithium ion batteries," *Ionics*, vol. 26, no. 3, pp. 1239–1247, Mar. 2020.

[41] H. Wu, H. Jile, Z. Chen, D. Xu, Z. Yi, X. Chen, J. Chen, W. Yao, P. Wu, and Y. Yi, "Fabrication of ZnO@MoS_2 Nanocomposite Heterojunction arrays and their photoelectric properties," *Micromachines*., vol. 11, no. 2, p. 189, 2020.

[42] J. Li, X. Chen, Z. Yi, H. Yang, Y. Tang, Y. Yi, W. Yao, J. Wang, and Y. Yi, "Broadband solar energy absorber based on monolayer molybdenum disulfide using tungsten elliptical arrays," *Mater. Today Energy*, vol. 16, Jun. 2020, Art. no. 100390.

[43] W. Li and Y. Cheng, "Dual-band tunable terahertz perfect metamaterial absorber based on strontium titanate (STO) resonator structure," *Opt. Commun.*, vol. 462, May 2020, Art. no. 125265.

[44] R. Dao, X. Kong, H.-F. Zhang, and X. Tian, "A tunable ultra-broadband metamaterial absorber with multilayered structure," *Plasmonics*, vol. 15, no. 1, pp. 169–175, Feb. 2020.

[45] Y. Guo, Y. Zhang, X. Chai, L. Zhang, L. Wu, Y. Cao, and L. Song, "Tunable broadband, wide angle and lithography-free absorber in the near-infrared using an ultrathin VO2 film," *Appl. Phys. Express*, vol. 12, no. 7, Jul. 2019, Art. no. 071005.

[46] X.-R. Kong, H.-F. Zhang, and R.-N. Dao, "A tunable ultra-broadband THz absorber based on a phase change material," *J. Electron. Mater.*, vol. 48, no. 11, pp. 7040–7047, Nov. 2019.

[47] J. Huang, J. Li, Y. Yang, J. Li, J. Li, Y. Zhang, and J. Yao, "Active controllable dual broadband terahertz absorber based on hybrid metamaterials with vanadium dioxide," *Opt. Express*, vol. 28, no. 5, p. 7018, Mar. 2020.

[48] T. Wang, Y. Zhang, H. Zhang, and M. Cao, "Dual-controlled switchable broadband terahertz absorber based on a graphene-vanadium dioxide metamaterial," *Opt. Mater. Express*, vol. 10, no. 2, p. 369, Feb. 2020.
[49] K. Niu, Q. Chen, R. Sun, B. Man, and H. Zhang, "Passively *Q*-switched erbium-doped fiber laser based on SnS_2 saturable absorber," *Opt. Mater. Express*, vol. 7, no. 11, pp. 3934–3943, Nov. 2017.
[50] J. Li, Z. Chen, H. Yang, Z. Yi, X. Chen, W. Yao, T. Duan, P. Wu, G. Li, and Y. Yi, "Tunable broadband solar energy absorber based on monolayer transition metal dichalcogenides materials using au nanocubes," *Nanomaterials*, vol. 10, no. 2, p. 257, 2020.
[51] Y. Nie, W. Xiao, C. Miao, M. Xu, and C. Wang, "Effect of calcining oxygen pressure gradient on properties of $LiNi_{0.8}Co_{0.15}Al_{0.05}O_2$ cathode materials for lithium ion batteries," *Electrochimica Acta*, vol. 334, Feb. 2020, Art. no. 135654.
[52] Y. Qi, C. Liu, B. Hu, X. Deng, and X. Wang, "Tunable plasmonic absorber in THz-band range based on graphene, 'arrow' shaped metamaterial," *Results. Phys.*, vol. 15, Dec. 2019, Art. no. 102777.
[53] C. Cen, Z. Chen, D. Xu, L. Jiang, X. Chen, Z. Yi, P. Wu, G. Li, and Y. Yi, "High quality factor, high sensitivity metamaterial Graphene—Perfect absorber based on critical coupling theory and impedance matching," *Nanomaterials*, vol. 10, no. 1, p. 95, 2020.
[54] M. Zhong, X. Jiang, X. Zhu, J. Zhang, J. Zhong, J. Chen, S. Wu, J. Zhang, L. Liang, L. Zeng, Y. Xin, and H. Chen, "Modulation of the absorption properties of a dual band metamaterial based on VO2 thin films," *Infr. Phys. Technol.*, vol. 104, Jan. 2020, Art. no. 103114.
[55] Y. Lv, Y. Li, C. Han, J. Chen, Z. He, J. Zhu, L. Dai, W. Meng, and L. Wang, "Application of porousbiomass carbon materials in vanadium redox flow battery," *J. Colloid Interface Sci.*, vol. 566, pp. 434–443, Apr. 2020.
[56] R. Naorem, G. Dayal, S. Anantha Ramakrishna, B. Rajeswaran, and A. M. Umarji, "Thermally switchable metamaterial absorber with a VO2 ground plane," *Opt. Commun.*, vol. 346, pp. 154–157, Jul. 2015.

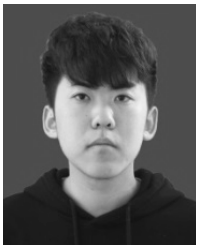

YUBING ZHANG received the B.S. degree in applied physics from Shijiazhuang University, Shijiazhuang, China, in 2018. He is currently a second-year Graduate Student majoring in physics with the Southwest University of Science and Technology, Mianyang, China. He was admitted to the Physics major of Southwest University of Science and Technology, in 2018. His research interests include the design and manufacture of micro/nano absorbers and terahertz metamaterial absorbers.

PINGHUI WU received the Ph.D. degree in optical engineering from Zhejiang University, China, in 2016. He is currently an Associate Professor with Quanzhou Normal University. His current research interests include the areas of nanophotonics, optical field manipulation and laser physics, and so on.

ZIGANG ZHOU received the Ph.D. degree in science from Suzhou University, in 2005. From July 1999 to July 2005, he worked as a Teacher at Southwest University, where he was engaged in optical teaching and scientific research. In August 2005, he joined the Southwest University of Science and Technology, where he is currently the Associate Dean and in charge of undergraduate teaching, experimental management, and optical teaching. His areas of research interest are micro-nano optics, integrated photonic devices, optical waveguide passive devices, and laser processing technology.

XIFANG CHEN received the B.S. degree from Guangxi Teachers Education University, the M.Sc. degree from Capital Normal University, and the Ph.D. degree in physical from Southeast University, Nanjing, Jiangsu. He is currently a Lecturer with the College of Science, Southwest University of Science and Technology. His research areas are nano luminescent materials and device physics.

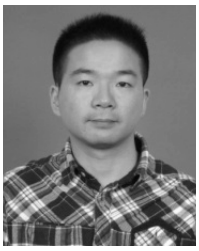

ZAO YI received the M.Sc. degree and the Ph.D. degree in condensed matter physics from Central South University, Changsha, Hunan, in 2010 and 2014, respectively. Since 2014, he has been with the Southwest University of Science and Technology, where he is currently a Professor of applied physics. His areas of research interest are plasmonics, nanophotonics, metamaterials, and their applications. He was a recipient of the Doctoral Academic Newcomer Awards of Ministry of Education, in 2012.

JIAYI ZHU received the Ph.D. degree in physical chemistry from the Technical Institute of Physics and Chemistry, CAS, China, in 2014. His research was in the field of self-assembly and optoelectronic property study of graphene-based nanostructured thin films. For two years, he worked as a Postdoctoral Researcher at the Research Center of Laser Fusion, CAEP, where he studied and designed carbon-based ultrablack materials. He is currently an Assistant Professor with the Southwest University of Science and Technology. His current research interests include areas of carbon-based optoelectronic nanostructured thin films and devices and so on.

TIANSHENG ZHANG received the Ph.D. degree in engineering from Gifu University, Japan, in 2012. Since October 2012, she has been a Lecturer with the College of Science, Huzhou University. From May 2016 to April 2017, she worked as a Visiting Scientist at the College of Engineering, Yamagata University, Japan. Her research areas are the synthesis of semiconductor materials and the application in solar cells.

HUGE JILE received the M.S. degree in project management from Hangzhou Dianzi University, China, in 2012. He is currently a Senior Experimentalist with Huzhou University. His current research interests include areas of optical materials, optical design and laser physics, and so on.